

Effects of intracellular Mn on the radiation resistance of the halophilic archaeon *Halobacterium salinarum*

Kimberly M. Webb · Jerry Yu · Courtney K. Robinson · Tomiya Noboru · Yuan C. Lee · Jocelyne DiRuggiero

Received: 22 December 2012 / Accepted: 7 March 2013 / Published online: 27 March 2013
© Springer Japan 2013

Abstract Ionizing radiation (IR) is of particular interest in biology because its exposure results in severe oxidative stress to the cell's macromolecules. Our recent work with extremophiles supports the idea that IR resistance is most likely achieved by a metabolic route, effected by manganese (Mn) antioxidants. Biochemical analysis of “super-IR resistant” mutants of *H. salinarum*, evolved over multiple cycles of exposure to high doses of IR, confirmed the key role for Mn antioxidants in the IR resistance of this organism. Analysis of the proteome of *H. salinarum* “super-IR resistant” mutants revealed increased expression for proteins involved in energy metabolism, replenishing the cell with reducing equivalents depleted by the oxidative stress inflicted by IR. Maintenance of redox homeostasis was also activated by the over-expression of coenzyme biosynthesis pathways involved in redox reactions. We propose that in *H. salinarum*, increased tolerance to IR is a combination of metabolic regulatory adjustments and the accumulation of Mn-antioxidant complexes.

Keywords Halophiles · Mn²⁺ · Oxidative stress · Ionizing radiation · Proteomics

Communicated by F. Robb.

Electronic supplementary material The online version of this article (doi:10.1007/s00792-013-0533-9) contains supplementary material, which is available to authorized users.

K. M. Webb · J. Yu · C. K. Robinson · T. Noboru · Y. C. Lee · J. DiRuggiero (✉)
Department of Biology, Johns Hopkins University,
3400 N. Charles St, Mudd Hall, Baltimore,
MD 21218, USA
e-mail: jdiruggiero@jhu.edu

Introduction

Ionizing radiation (IR) is highly detrimental to biological systems and most of the damage to cellular components results from radiolysis of water and the production of reactive oxygen species (ROS) such as hydroxyl radicals (HO·), superoxide (O₂⁻) and hydrogen peroxide (H₂O₂) (Riley 1994). While ROS damage DNA through base modification, strand breaks and cross-linking with proteins, evidence suggests that the most threatening damage is to proteins, resulting in carbonylation of protein residues, oxidation of the backbone, and ultimately protein inactivation and denaturation (Imlay 2003; Daly 2009). The most susceptible proteins contain exposed iron–sulfur groups, where O₂⁻ and H₂O₂ can cause the release of ferrous ions (Fe²⁺) in the cytoplasm, enzyme inactivation, and the failure of metabolic pathways (Imlay 2006). The released Fe²⁺ participate in Fenton chemistry, generating additional HO· and inflicting additional oxidative damage to macromolecules (Imlay 2008).

In radiation-resistant microorganisms, the damage inflicted by IR must either be avoided, repaired, or both in order for cells to survive (Daly 2009; Robinson et al. 2011). While DNA repair systems in IR-resistant bacteria continue to be scrutinized, recent work with *Deinococcus radiodurans* showed that the DNA repair proteins involved were not unique to IR-resistant bacteria (Slade et al. 2009; Confalonieri and Sommer 2011; Daly 2012). In the Archaea, mutants of *Halobacterium salinarum* deficient in the homologous recombination proteins Rad50 and Mre11 ($\Delta rad50$ – $\Delta mre11$) are just as IR-resistant as the wild-type, though the repair of DNA double-strand breaks (DSBs) occur less efficiently (Kish and DiRuggiero 2008). These facts together with the demonstration that IR-sensitive and IR-resistant organisms suffer the same number of DNA

DSBs for an equivalent dose of IR (~ 0.04 DSB/Gy/Mbp) depart from the dogma that DNA damage, and in particular DNA DSBs, are the most cytotoxic lesions resulting from exposure to IR (Daly 2009). A number of studies (Du and Gebicki 2004; Nauser et al. 2005; Daly et al. 2007) have now established that proteins are the major targets for oxidation following exposure to IR. In the current model, it is the ability of cells to protect their proteins from IR-induced oxidation that promotes repair functions, genome restoration, and cell survival (Daly 2012).

Major defenses of the cell against oxidative stress from exposure to H_2O_2 and redox cycling drugs—producing superoxide—are enzymatic (Imlay 2008). Surprisingly, superoxide dismutase (SOD) and catalase knockout mutants of *H. salinarum* showed the same level of survival to IR as wild-type (Robinson et al. 2011), suggesting that these enzymes were not required for *H. salinarum* IR survival; similar results were also obtained with the bacteria *D. radiodurans* and *E. coli* (Markillie et al. 1999; Scott et al. 1989). In addition, in bacterial systems and in *H. salinarum*, SODs and catalases were induced by several orders of magnitude in response to redox cycling drugs and H_2O_2 (Kaur et al. 2010), but no increase in mRNA or protein levels for SODs, catalases, or peroxidases was detected in *H. salinarum* after exposure to IR (Whitehead et al. 2006). In place of enzymatic defense systems, a number of studies have underlined the key role played by Mn-antioxidant complexes in the scavenging of ROS and the protection of cellular macromolecules from IR-induced oxidative damage. For example, high levels of Mn were found to substitute for the lack of SOD in *Lactobacillus plantarum* (Archibald and Fridovich 1982) and to rescue SOD-deficient mutants of *E. coli* and *Saccharomyces cerevisiae* (Chang and Kosman 1989; Al-Maghrebi et al. 2002). Mn(II) associated with phosphate, pyrophosphate, and small organic molecules has been shown to exhibit superoxide-scavenging activity in vitro (Archibald and Fridovich 1982; Barnese et al. 2008; Chang and Kosman 1989). More recently, Mn-phosphate complexes together with nucleosides, small peptides, or trehalose were shown to protect enzyme activity, in vitro, against the deleterious effect of IR (Daly et al. 2010; Webb and DiRuggiero 2012; Robinson et al. 2011). Furthermore, the high Mn/Fe ratio found in IR-resistant microorganisms revealed a direct link between Mn and the protection of proteins from oxidative damage by ROS (Fredrickson et al. 2008; Daly 2009; Kish et al. 2009). Work with *D. radiodurans* elegantly established the key role played by Mn-peptide complexes in the extreme radiation resistance of this organism (Daly et al. 2010) and in yeast, in vivo studies showed the important function of Mn-orthophosphate complexes in oxidative stress (McNaughton et al. 2010). In addition to its antioxidant activity, Mn may also act by functionally substituting

for Fe in the Fe–S cluster of enzymes and thereby alleviating the deleterious effects of Fenton chemistry during oxidative stress (Sobota and Imlay 2011).

The halophilic archaeon *H. salinarum* grows optimally at 4 M NaCl and accumulates equimolar amounts of KCl for osmotic balance. In its natural environment, it is exposed to a number of oxidative stressors that include UV radiation and cycles of desiccation and rehydration (DasSarma and Arora 2001). This well-characterized halophile is extremely resistant to desiccation, radiation, and pressure (Kottemann et al. 2005; Kish et al. 2012) and our work showed that *H. salinarum* enzyme-free cell extracts rich in Mn, phosphate (PO_4), and amino acids provided a great level of protection for protein activity against the deleterious effect of IR (Robinson et al. 2011). DeVeaux et al. (2007) selected super radiation-resistant mutants of *H. salinarum* after multiple rounds of high-level IR to explore the potential for increasing IR resistance in this archaeon. A similar type of strain evolution was previously done with *E. coli* and *Salmonella typhimurium* LT2 (Davies and Sinskey 1973; Harris et al. 2009). Using a similar method, we selected for super-radiation (IR^+) isolates of *H. salinarum* to investigate the metabolic routes instrumental to enhanced IR resistance. Our proteomic-based approach was complemented with biochemical analyses of the IR^+ isolates and the metabolites they accumulate. Our findings indicate that increased tolerance to IR is a combination of metabolic regulatory adjustments and the accumulation of Mn-antioxidant complexes.

Materials and methods

Strains and culture conditions

Halobacterium salinarum (ATCC 700922) Δ *ura3* and IR^+ isolates were grown in standard GN101 medium (250 g/l NaCl, 20 g/l $MgSO_4 \cdot 7H_2O$, 2 g/l KCl, 3 g/l Na citrate, 10 g/l Oxoid-brand peptone), pH 7.2, with the addition of 1 ml/l trace element solution (31.5 mg/l $FeSO_4 \cdot 7H_2O$, 4.4 mg/l $ZnSO_4 \cdot 7H_2O$, 3.3 mg/l $MnSO_4 \cdot 7H_2O$, 0.1 mg/l $CuSO_4 \cdot 5H_2O$) and supplemented with a final concentration of 50 mg/l uracil (Sigma, St. Louis, MO, USA). Cultures were grown at 42 °C with shaking at 220 rpm (Innova 4080 incubator shaker, New Brunswick Scientific, Edison, NJ, USA).

Selection of IR^+ isolates

Single-picked colonies were grown in GN101 supplemented with uracil to an OD of 0.4 at 600 nm (mid exponential phase of growth) and irradiated in their growth medium at the indicated doses with a ^{60}Co gamma source

(dose rate = 3.2 kGy/h; Uniformed Services University of the Health Sciences, Bethesda, MD, USA), as described before (Robinson et al. 2011). Immediately following irradiation, cells were (1) tested for survival as described below and (2) inoculated into fresh media, grown to an OD of 0.4 at 600 nm, and stored in 15 % glycerol at -80°C . We found that 0.0035–0.01 % of the cells survived irradiation at 23 kGy, depending the irradiation round and the founder from which they were evolved. For each subsequent irradiation, cultures were grown from their glycerol stocks to an OD of 0.4 at 600 nm prior to irradiation. Cultures were irradiated at doses up to 23 kGy (Fig. S1). At the end of 6–9 rounds of IR, single-picked colonies from each IR⁺ cultures were grown to OD 0.8 (late exponential phase) and stored in 15 % glycerol at -80°C . Survival tests using 12 kGy as a benchmark were carried out on all cultures and isolates. All isolates were derived from 3 founder strains, F1, F2, and F3, and designated as “Founder-Final Round IR-Isolate #.” For example, the IR⁺ isolate 392 was the isolate #2 after 9 rounds of IR of Founder 3.

Survival assays

Following irradiation at the indicated doses, *H. salinarum* cultures were serially diluted in Basal Salt Solution (BSS; 250 g/l NaCl, 20 g/l MgSO₄·7H₂O, 2 g/l KCl, 3 g/l Na citrate) and plated on GN101 supplemented with 50 mg/l uracil. Plates were incubated at 42 °C for 5–7 days. Survival was expressed as the number of colony forming units (CFUs) following treatment divided by the number of CFUs without treatment. For each isolate and F3, the survival rate was calculated as the average of 3 independent experimental replicates which were 3 cultures independently grown, each from a single colony. The survival rate for each independently grown culture was determined by plating the control and irradiated cultures in triplicates. Standard errors were calculated using the means of 3 independent experiments with 3 measurements each. A *t* test was used to test statistical significance.

Preparation of protein-free cell extracts (ultrafiltrates, UFs)

Halobacterium salinarum cultures were grown to an OD of 0.4 at 600 nm, and harvested cells were washed twice with BSS. Pellets were re-suspended in distilled and deionized water (ddH₂O; Sigma-Aldrich, St. Louis, MO, USA) and passed through an Emulsiflex Homogenizer (Avestin, Inc., Ottawa, Canada) at 15,000 psi to lyse the cells. The cell extracts were centrifuged at 12,000×*g* (60 min, 4 °C) and standardized by protein concentration, which was determined by the BioRad Bradford Assay (BioRad, Hercules,

CA, USA). The supernatant was further centrifuged at 190,000×*g* (40 h, 4 °C) and then subjected to filtration using 3 kDa centrifugal devices (Amicon ultracel 3 k filters; Millipore, Billerica, MA, USA). The resulting ultrafiltrates (UFs) were concentrated 5 times in a speed vacuum concentrator (Heto Vacuum Centrifuge; ATR, Laurel, MD, USA). Samples were aliquoted and stored at -20°C .

Enzyme protection assays

The restriction enzyme *DdeI* was added at a final concentration of 0.5 U/μl to UFs diluted to 0.2×. The solutions were irradiated using a ⁶⁰Co gamma source (Uniformed Services University of the Health Sciences, Bethesda, MD, USA; dose rate = 3.2 kGy/h) up to 12 kGy. Samples were kept on ice until digestion of 1 μg of pUC19 DNA using 1 U of enzyme from each irradiated solution at 37 °C for 1 h. The resulting pUC19 DNA fragments were separated by electrophoresis on 1 % agarose TBE gels and visualized with ethidium bromide staining, and imaged using BioDoc-ItTM Imaging System (UVP, LLC, Upland, CA, USA).

Determination of amino acid concentration

Free and total amino acid concentrations in the *H. salinarum* UFs were determined using the ninhydrin assay as described before (Robinson et al. 2011). Analyses were performed with 3 independently made UFs, with triplicate measurements.

Amino acid analysis

The UFs underwent Fmoc-derivatization in parallel with a 17 standard amino acid mixture (Sigma-Aldrich, St. Louis, MO, USA). In brief, 2 μl of sample or standard was added to 2 μl L-norleucine and 6 μl water, diluted 10-fold in 0.1 M sodium bicarbonate-HCl buffer (pH 7.7). 100 μl of 10 mM acetonitrile Fmoc-Cl (Sigma-Aldrich, St. Louis, MO, USA) was added, vortexed, and incubated at room temperature for 1 min. Excess Fmoc-OH was extracted with *n*-hexane (1 ml) 10 times. Aqueous layer was recovered and diluted 100-fold with 50 mM sodium acetate (pH 4.2). 10 μl was injected onto a YMC-Triart C18 column (1.9 μm, YMC Co., Ltd.) using a Nexera SIL-30AC with RF-20AxS fluorescence detector (Shimadzu Scientific Instruments, Columbia, MD, USA) at 264 nm. Eluent A: 4:1 mixture of 50 mM sodium acetate and acetonitrile; eluent B: 1:10 mixture of 50 mM sodium acetate and acetonitrile. A concave gradient of 90 % eluent A, 10 % eluent B to 100 % eluent B over 60 min was used. Flow rate was 0.8 ml/min.

ICP-MS and ion chromatography

Mn, Fe, and PO₄ concentrations in *H. salinarum* UFs and cells (Mn, Fe) were determined using ICP-MS (Mn, Fe) and ion chromatography (PO₄) at the Division of Environmental Health Engineering, JHU School of Public Health as described previously (Robinson et al. 2011). Analyses were performed with 3 independently made UFs or 3 independently grown cultures, with triplicate measurements.

Protein extraction and precipitation

Cultures were grown in duplicates to an OD of 0.4 at 600 nm and cells were harvested by centrifugation 8,000×g (10 min, 4 °C). Cell pellets were re-suspended in ice-cold salt buffer (50 mM potassium phosphate pH 7.0, 1 M NaCl, 1 % 2-mercaptoethanol) and subjected to three cycles of sonication for 30 s (Virsonic 100; Virtis, Gardiner, NY, USA) followed by incubation on ice for 30 s. Cell lysates were then fractionated by centrifugation (8,000×g, 30 min, 4 °C), with the supernatant withdrawn and stored at –20 °C. Protein concentration was determined by the BioRad Bradford Assay (BioRad, Hercules, CA, USA). Aliquots containing 200 µg of protein were stored on ice and 8 volumes of –20 °C TCA/acetone were added. The mixture was vortexed briefly, incubated at –20 °C for 4 h, and then pelleted by centrifugation (16,000×g, 10 min, 0 °C) before discarding the supernatant and air-drying the pellet. Protein yield was measured by subjecting another aliquot of 200 µg to the same protocol and by re-suspending the pellet in one volume of denaturing buffer (50 mM potassium phosphate pH 7.0, 1 M NaCl, 1 % 2-mercaptoethanol, 6 % sodium dodecyl sulfate) before measuring protein concentration the Bradford Assay. To verify that the TCA/acetone precipitation process did not result in a loss of a significant amount of proteins, denatured proteins from both TCA-treated and non-TCA-treated extracts were separated by denaturing acrylamide gel electrophoresis (SDS-PAGE) on a 4–20 % gradient gel at 150 V, 60 mA for 1.5 h. The gel was stained with Bio-Rad Flamingo™ stain (BioRad, Hercules, CA, USA) and imaged using BioDoc-It™ Imaging System (UVP, LLC, Upland, CA, USA) and Typhoon (GE Healthcare Life Science, Piscataway, NJ, USA).

Protein digestion, iTRAQ labeling, and LC–MS analysis

The TCA/acetone-precipitated protein pellets were re-suspended in 20 µl 500 mM TEAB (triethyl ammonium bicarbonate) and 1 µl 2 % SDS. Each sample was reduced by adding 2 µl 50 mM TCEP [tris-(2-carboxyethyl)

phosphine] for 1 h at 60 °C, alkylated by 1 µl 200 mM MMTS (methyl methanethiosulfonate) for 15 min at room temperature, then digested at 37 °C overnight with trypsin (Promega, Fitchburg, WI, USA) using a 1:10 enzyme to protein ratio. Samples were labeled by adding 100 µl of an iTRAQ reagent (Applied Biosystems, Foster City, CA, USA) dissolved in isopropanol and incubated at room temperature for 2 h. All samples were dried to a volume of approximately 30 µL and subsequently mixed. The combined peptide sample was dissolved in 8 mL of SCX loading buffer (25 % v/v acetonitrile, 10 mM KH₂PO₄, pH 2.8) and subsequently fractionated by strong cation exchange (SCX) chromatography on an Agilent 1200 Capillary HPLC system (Agilent Technologies, Santa Clara, CA, USA) using a PolySulfoethyl A column (2.1 × 100 mm, 5 µm, 300 Å) (PolyLC, Columbia, MD, USA). The sample was loaded and washed isocratically with 25 % v/v acetonitrile, 10 mM KH₂PO₄, pH 2.8 for 40 min at 250 µl/min. Peptides were eluted and collected in 1 min fractions using a 0–350 mM KCl gradient in 25 % v/v acetonitrile, 10 mM KH₂PO₄, pH 2.8, over 40 min at 250 µl/min, monitoring elution at 214 nm. The SCX fractions were dried, re-suspended in 200 µl 0.05 % TFA and desalted using an Oasis HLB uElution plate (Waters, Milford, MA, USA). Desalting peptides were loaded for 15 min at 750 nl/min directly on to a 75 µm × 10 cm column packed with Magic C18 (5 µm, 120Å, Michrom Bioresources, Auburn, CA, USA). Peptides were eluted using a 5–40 % B (90 % acetonitrile in 0.1 % formic acid) gradient over 90 min at 300 nl/min. Eluting peptides were sprayed directly into an LTQ Orbitrap Velos mass spectrometer (ThermoScientific, Waltham, MA, USA) through an 1 µm emitter tip (New Objective, Woburn, MA, USA) at 1.6 kV. Survey scans (full ms) were acquired from 350 to 1,800 *m/z* with up to 10 peptide masses (precursor ions) individually isolated with a 1.2 Da window and fragmented (MS/MS) using a collision energy of 45 and 30 s dynamic exclusion. Precursor and the fragment ions were analyzed at 30,000 and 7,500 resolution, respectively.

Data analysis

The MS/MS spectra were extracted and searched against the GenBank database using Mascot (Matrix Science, Boston, MA, USA) through Proteome Discoverer software (ThermoScientific, Waltham, MA, USA) specifying sample's species, trypsin as the enzyme allowing one missed cleavage, fixed cysteine methylthiolation and 8-plex-iTRAQ labeling of N-termini, and variable methionine oxidation and 8-plex-iTRAQ labeling of lysine and tyrosine. Peptide identifications from Mascot searches were processed within the Proteome Discoverer to identify peptides with a confidence threshold 1 % false discovery

rate (FDR), based on a concatenated decoy database search. A protein's ratio is the median ratio of all unique peptides identifying the protein at a 1 % FDR.

Results

Enrichment and selection of IR⁺ isolates

We selected for super IR-resistant (IR⁺) isolates of *H. salinarum* to further investigate the mechanisms contributing to the radiation resistance of this halophile. Five individual cultures (founders F1–F5) were sequentially irradiated with high levels of gamma-radiation (Fig. S1). After completion of the irradiation-recovery rounds (9 rounds for cultures F1, F2 and F3, and 6 rounds for cultures F4 and F5), a survival test using 12 kGy as a benchmark showed 60 % survival for cultures IR2-9, IR4-6, and IR5-6, and 42 and 23 % survival for cultures IR1-9 and IR3-9, respectively (Fig. S2). Thirty isolates were randomly selected and tested for their survival at 12 kGy; survival for 23 of the 30 isolates was higher than 50 % and all had significant increases in IR resistance when compared to the founder (F3) strain (Fig. S3). Isolates 392, 393 and 463 were selected for further investigation; Founder 3 was used for comparison. The D₁₀—the dose at which 10 % of the cells survive—was calculated from survival curves for each of the 3 isolates and revealed an increase from 5 to 17 kGy when compared with F3 and with previous values for wild-type *H. salinarum* (Fig. 1) (Kottemann et al. 2005).

Ultrafiltrate protection of enzyme activity from radiation

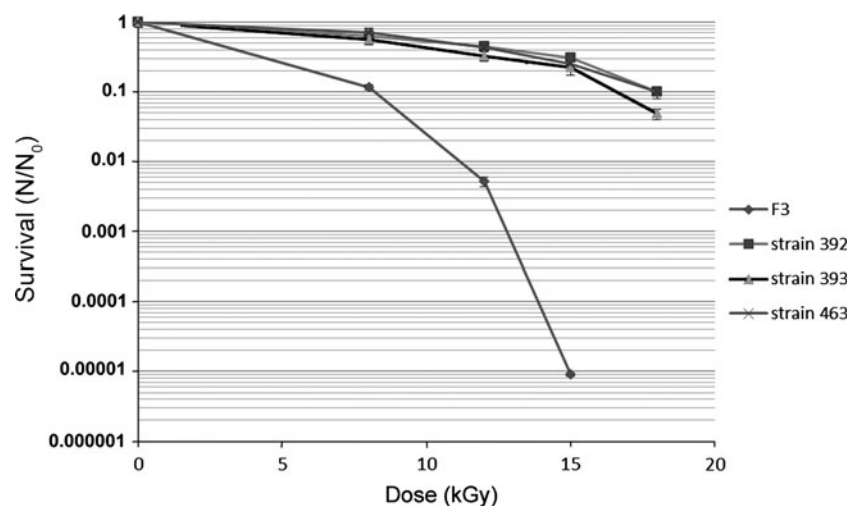
To determine the role of antioxidant molecules in the increased IR resistance of *H. salinarum* IR⁺ isolates, we

tested the ability of enzyme-free cell extracts (UFs) from isolates 392, 393 and 463, and from F3, to protect enzyme activity from IR, in vitro. The restriction enzyme *DdeI* was irradiated at increasing doses of gamma ray, in presence of the UFs, and its residual activity determined by restriction of plasmid DNA and analysis of the fragments by gel electrophoresis. Residual enzyme activity was detected up to 6 kGy with UF_{F3} and up to 10–12 kGy with UFs from the 3 IR⁺ isolates, demonstrating significant increase in IR protection in vitro (Fig. 2). While we observed a loss of cleavage site specificity for the enzyme at the highest doses, the doses at which this and the total loss of protein activity occurred were consistent across the IR⁺ isolates and F3.

Biochemical composition of ultrafiltrates

Accumulation of intracellular manganous (Mn²⁺) ions forming antioxidant complexes with peptides, orthophosphate, and other small molecules, and catalytically scavenging ROS, was previously demonstrated for *H. salinarum* and *D. radiodurans* (Daly et al. 2010; Robinson et al. 2011). We therefore measured the concentrations of Mn, PO₄, and amino acids in our 3 IR⁺ isolates. Isolates 392 and 463 had 1.5-fold and 1.3-fold increased Mn in their UFs, respectively, when compared to UF_{F3} ($p < 0.05$; Fig. 3a), and UF₃₉₂ had 1.5-fold more PO₄ and 2.5-fold more amino acids than UF_{F3} ($p < 0.05$; Fig. 3b, c). Compositional analysis of amino acids showed that the concentration of glycine in UF₃₉₂ was 3 times that UF_{F3} (Fig. 3d). The UF from isolate 393 had concentration of Mn, PO₄, and amino acids comparable to that of F3 (Fig. 3). We next used a proteomic analysis to investigate changes in protein abundances in IR⁺ isolates with respect to F3 and to identify proteins and metabolic pathways that contributed to the enhanced IR resistance observed in these isolates.

Fig. 1 Survival of IR⁺ isolates and founder strain F3 at increasing doses of ionizing radiation. Survival was calculated as the average ratio (N/N_0) of surviving CFU from treated (N) compared to untreated (N_0) cultures. Data are the averages of three independent experiments with triplicate measurements each; standard errors shown



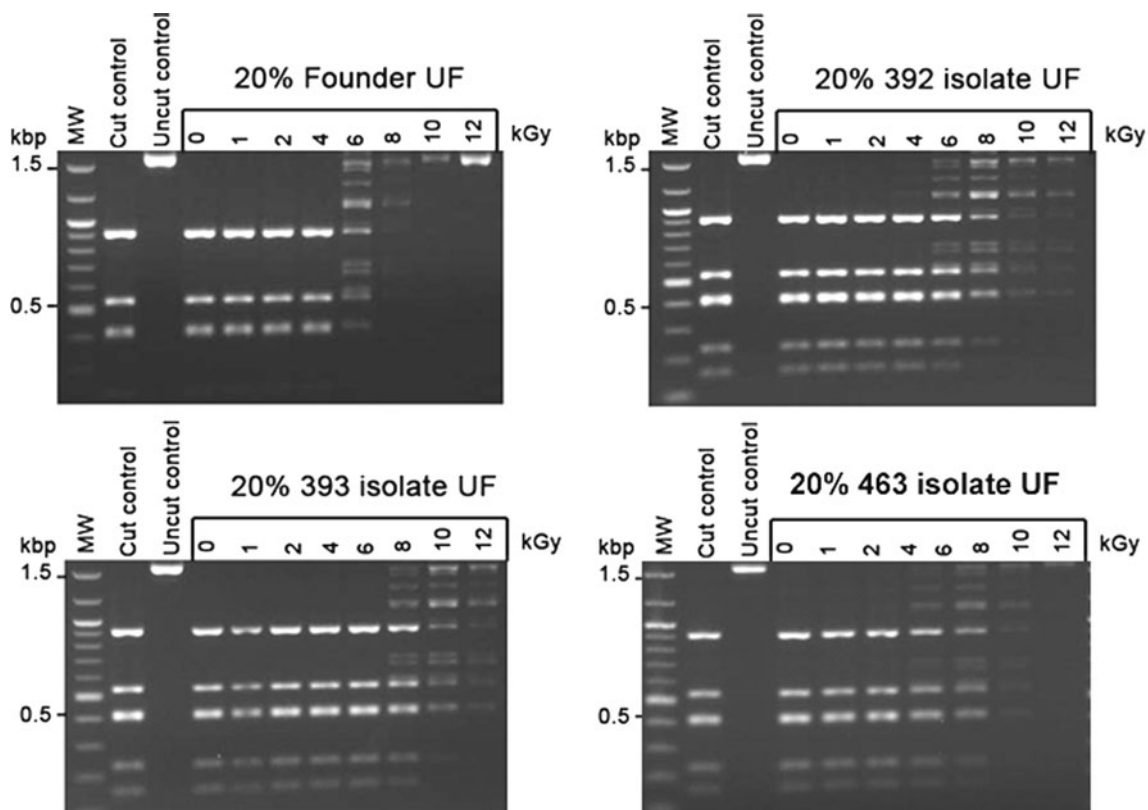


Fig. 2 Protection of enzyme activity. The restriction enzyme *DdeI* was irradiated up to 12 kGy in UFs of *H. salinarum* IR⁺ isolates and founder strain F3. Residual restriction enzyme activity was assayed

by the digestion of pUC19 plasmid DNA. Fragments were analyzed by agarose gel electrophoresis. The *first lanes* are molecular size ladders

Data validation for proteomic analysis

We used isobaric tags for relative and absolute quantitation (iTRAQ) to analyze differential protein expression in the IR⁺ isolates 392, 393, 463, and founder F3. In order to determine the steady-state protein expression levels in each isolate, cells were harvested without irradiation and grown under optimal conditions. iTRAQ analysis of the proteins from the IR⁺ isolates and F3-produced 386,843 spectra. Using the GenBank database, we identified 126,845 peptides that formed 1,266 protein groups and 1,279 merged proteins, covering 48 % of the *H. salinarum* proteome.

We compared the physical properties of proteins identified in our iTRAQ dataset with predicted values of the *H. salinarum* proteome to check for biases (data obtained from the Comprehensive Microbial Resource database, CMR, <http://cmr.jvci.org/tigr-scripts/CMR/CmrHomePage.cgi>). The predicted proteome of *H. salinarum* had a mean molecular weight of 31.5 kDa and a median molecular weight of 27.6 kDa. The iTRAQ-identified proteins ranged in molecular weight from 10 to 50 kDa, with a mean and median of 34.1 and 29.7 kDa, respectively (Fig. S4a). With respect to isoelectric point (*pI*), the calculated *pI* for iTRAQ-identified proteins had a mean and median of 4.79 and

4.59, respectively (Fig. S4b). These values are close to a median of 4.9 that was previously predicted for the *H. salinarum* proteome (Kennedy et al. 2001). Both the molecular weights and the *pI* values of our iTRAQ-identified proteins indicated that our dataset was a good representation of the *H. salinarum* proteome without notable biases.

Using the classification from the CMR database, we sorted the iTRAQ-identified proteins and the *H. salinarum*-predicted proteome into 18 metabolic categories, which included distinction for hypothetical, unclassified, and proteins of unknown function (Fig. S5). In both datasets (identified and predicted), hypothetical and unclassified proteins were the largest categories, and for proteins of known function, energy metabolism out-numbered all other processes (Fig. S5). The iTRAQ-identified proteins correlated with the predicted proteome for all the categories, save for under-representation of cell envelope and transport proteins (Fig. S5).

Using Proteome Discoverer, protein expression ratios (PER) were calculated for each protein using unique MS-identified peptides for each protein and an overall assigned score. This score (A4 score) was the sum of the absolute probabilities for the unique peptides identifying the protein.

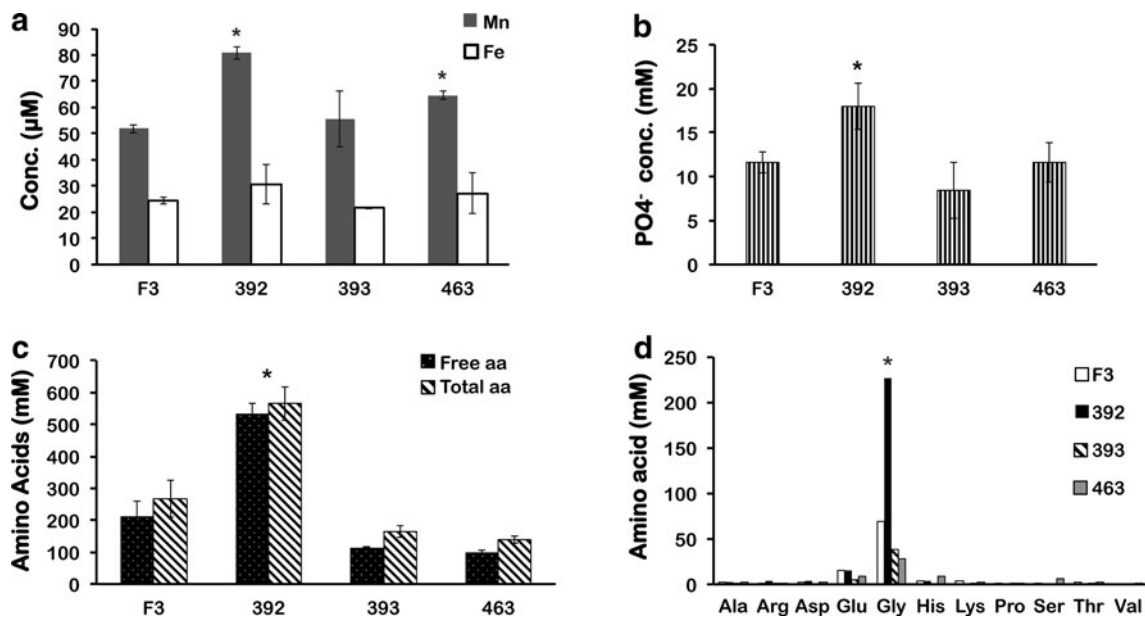


Fig. 3 Mn and Fe (a), phosphate (b), total and free amino acids (c), and amino acid composition (d) measured in the enzyme-free UFs of *H. salinarum* IR⁺ isolates and founder strain F3. Data for a–c are the

averages of at least three experimental replicates with triplicate measurements each; standard errors shown

A threshold of >100 A4 score was used to remove proteins with poor peptide coverage (determined using Proteome Discoverer). Ratios of protein expression (PER) between biological replicates were close to one whereas ratios between each of the IR⁺ isolates (392, 393 and 463) and F3 ranged from 1 to 6.9, representing proteins differentially expressed in the IR-evolved isolates when compared to the founder strain (Fig. S6).

Differential protein expression in IR⁺ isolates

We identified proteins differentially expressed in the IR⁺ isolates with respect to the founder by selecting cut-off ratios of <0.4 and >1.5 for a FDR of <6 %. FDR were calculated by computing outliers in all biological replicate comparisons at specific cut-off ratios. A FDR of 6 % indicates that there is less than 6 % chance that the expression level of a protein was not significantly increased or decreased at ratios above 1.5 or below 0.4, respectively. Protein expression ratios (PER) between the four possible permutations for each isolate (isolate-1 with F3-1; isolate-2 with F3-1; isolate-1 with F3-2; and isolate-2 with F3-2) were averaged and PER <0.4 were deemed as decreased protein expression, whereas PER >1.5 were deemed as increased protein expression with respect to F3 (Tables S1 and S2).

Decreased protein expression ratios in IR⁺ isolates

We found a total of 14 proteins with decreased PER and they fell into 4 functional categories: transcription,

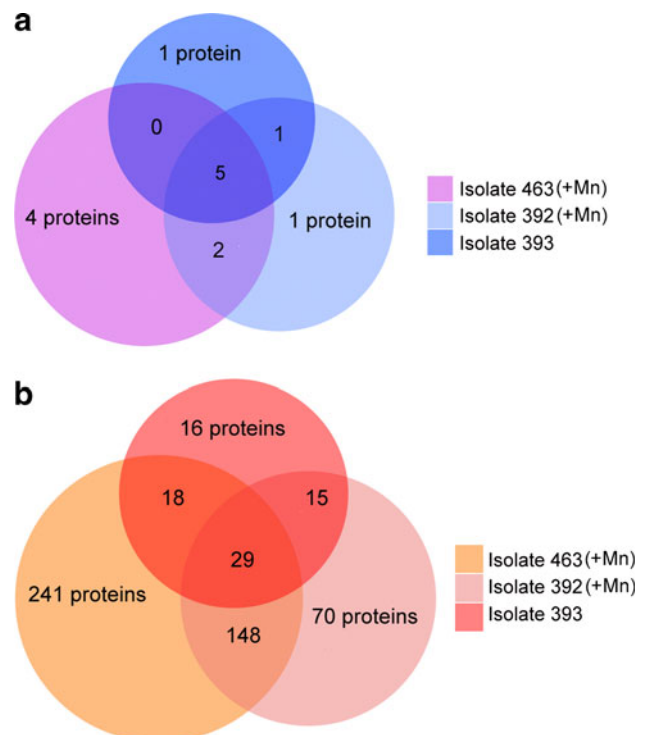


Fig. 4 Numbers of proteins with decreased (a) and increased (b) protein expression ratios (PER) identified in IR⁺ isolates by the iTRAQ proteomic analysis. Isolates 392 and 463 had elevated Mn concentration in their UFs when compared to the founder strain F3

regulation, cellular processes, and unknown (Fig. 4a, Table S1). Five of the 14 proteins were common to the 3 IR⁺ isolates, including 3 gas vesicle proteins GvpC, GvpN, and

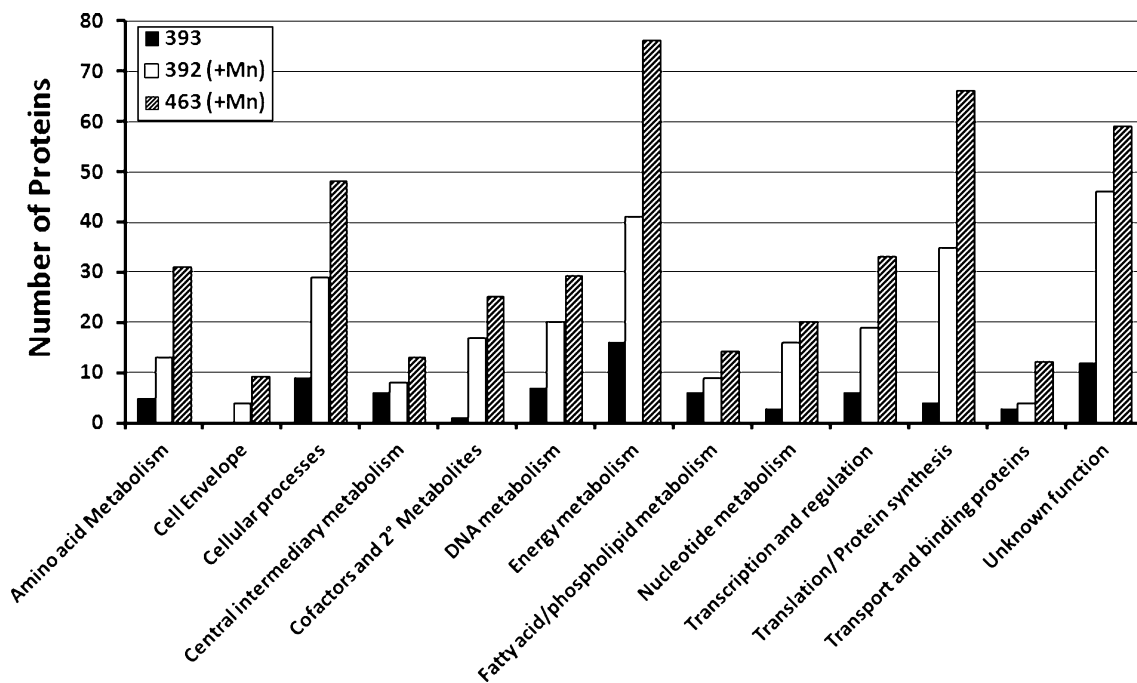


Fig. 5 Classification of protein metabolic functions for over-expressed proteins in IR⁺ isolates. Isolates 392 and 463 had elevated Mn concentration in their UFs when compared to the founder strain F3

GvpO (VNG7026, VNG7027, and VNG7028), a chromosome partitioning protein SojB (VNG7029), and a putative signal-transducing histidine kinase/response regulator protein HtlD (VNG7030), all located on plasmid pNRC100. The decreased PER for gas vesicle proteins in the IR⁺ isolates indicated a deficiency in gas vesicles biogenesis, confirmed by the sinking phenotype observed for the 3 isolates (Kaur et al. 2010), and providing an experimental validation of our iTraQ dataset. Because the three IR⁺ isolates we characterized were gas vesicle-deficient, we tested whether the loss of gas vesicles contributed to the enhanced IR⁺ resistance of these strains. A spontaneous F3*vac*⁻ mutant was isolated and its radiation resistance compared to that of F3. We found no significant difference in IR resistance between the F3*vac*⁻ mutant and F3, suggesting that the loss of gas vesicles did not contribute to increased IR⁺ resistance in these strains (Fig. S7).

Increased protein expression ratios in IR⁺ isolates

Five hundred and thirty seven proteins had increased PER and 29 of those were common to all IR⁺ isolates (Fig. 4b; Table S2). These included a ArgK-type transport ATPase (VNG0674C), 2 single-strand DNA binding proteins (Rfa3, Rfa8), threonine synthase (VNG2430G), both superoxide dismutases (Sod1, Sod2), a cell division cycle protein (Cdc48b), a general stress protein 69 (Gsp), glyceraldehyde-3-phosphate dehydrogenase (GapB), phosphoenolpyruvate synthase (PpsA), a carboxypeptidase (Cxp), 2-oxoglutarate

ferredoxin oxidoreductase subunit alpha (PorA), and V-type ATP synthase subunit E (VNG2142) (Table S2). Isolate 463 had the highest number of proteins with increased PER among the 3 isolates, 435 proteins, whereas isolate 392 had 262, and 393 had 78 proteins, respectively (Fig. 4b). Excluding the 29 proteins in common to all isolates, 463 had 148 proteins with increased PER in common with isolate 392 but only 19 with isolate 393 (Fig. 4b). The 19 proteins in common between 463 and 393 included a flavin-dependent oxidoreductase (Mer), phosphoglycerate dehydrogenase (SerA3), alcohol dehydrogenase (Adh2), and a putative glutathione S-transferase (VNG2281C) (Table S2).

To further investigate proteins with increased PER, proteins were manually evaluated for further annotation and plotted according to the CMR database metabolic categories for each IR⁺ isolate. Several categories from the CMR database were combined to better visualize trends in protein functions, i.e. “Transcription” and “Regulation” were combined, “Protein Synthesis” and “Translation” were combined, “Biosynthesis of Cofactors” and “Prosthetic Groups and Carriers” were annotated as “Cofactors and 2° Metabolites”, and “Hypothetical”, “Unclassified” and “Unknown” were combined into “Unknown” (Fig. 5). Isolates 392 and 463 shared the same trend with the highest number of over-expressed proteins associated with energy metabolism, cellular processes, cofactor biosynthesis, and translation/protein synthesis. Thirty-two of the 177 proteins in common between 392 and 463 were classified as energy metabolism proteins and included phosphoglyceromutase

(GpM), a cytochrome-like protein (Fbr), phosphopyruvate hydratase (Eno), NADH oxidase (NoxA), phosphoglycerate kinase (Pgk), fructose-bisphosphate aldolase (Fbp), and a pyruvate dehydrogenase component (Dsa) (Table S2). “Cellular processes” was also a dominant category for common over-expressed proteins between isolates 392 and 463 with a hypothetical peptidase (VNG0437C), a heat shock protein (Hsp2), 2 chemotaxis proteins (CheW1, CheC1), and 2 cell division proteins (FtsZ3, FtsZ4). There were 7 proteins related to cofactor biosynthesis in common between isolates 392 and 463, including two NAD synthesis proteins, L-aspartate oxidase (NadB) and NAD synthetase (NadE). The majority of proteins associated with translation/protein synthesis were ribosomal proteins suggesting up-regulation of protein synthesis (Table S2). One of 2 transport proteins with increased PER common to isolates 392 and 463 was a hypothetical K⁺ transport system (VNG0983C) that could potentially bind Mn (UniProtKB/TrEMBL: Q9HQW0). This is notable because both isolates 392 and 463 had increased intracellular Mn, with respect to F3, but not isolate 393 (Fig. 3a).

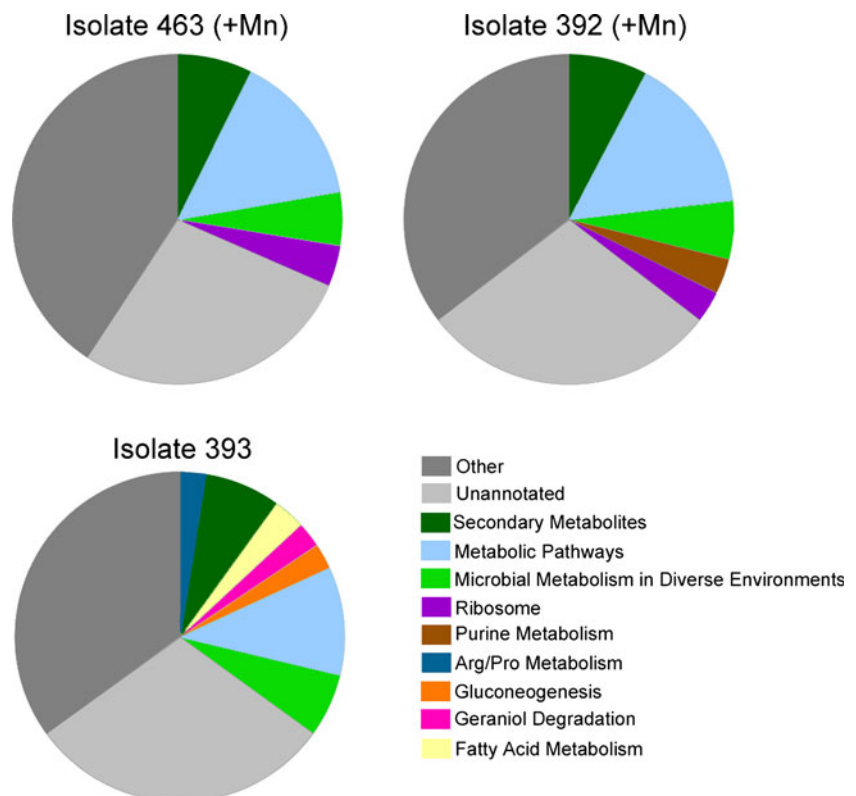
We found 239 proteins with increased PER that were unique to isolate 463. These included 8 peptidases, 6 universal stress response proteins, 7 proteins associated with oxidative phosphorylation, and a starvation-induced DNA-binding protein (DpsA) (Table S2). Among the proteins with increased PER that were unique to isolate 392, 4 are

involved in the NAD synthesis pathway, quinolinate synthetase (NadA), nicotinate-nucleotide pyrophosphorylase (NadC), NadB, and NadE. In addition, the average PER for NadA, NadB, and NadC were 5.0, 6.9, and 3.2, respectively, and were among the highest values for isolate 392.

We also found 15 over-expressed proteins in common between isolates 392 and 393, including a bacterio-opsin linked protein (VNG1463), a NADH dehydrogenase/oxidoreductase-like protein (VNG1932), an acyl-CoA dehydrogenase (VNG1191), and a photolyase/cryptochrome protein (Phr1) (Table S2). The distribution of metabolic categories for over-expressed proteins in isolate 393 differed from that of isolates 392 and 463; most over-expressed proteins for 393 belong to categories for energy metabolism, cellular processes, unknown function, and DNA metabolism, with a small number related to cofactor biosynthesis and none to cell envelope functions (Fig. 5). Proteins with increased PER unique to isolate 393 included a serine protein kinase (Prk), a transcription regulator (Trh5), a TRK potassium uptake system protein (VNG1924G), and a phytoene dehydrogenase (VNG1755G).

The correlation between high intracellular Mn and overall metabolic trends of over-expressed proteins between isolates 392 and 463 was investigated by classifying over-expressed proteins according to the KEGG (Kyoto Encyclopedia of Genes and Genomes) metabolic pathways (Fig. 6). Similar over-expressed metabolic

Fig. 6 KEGG pathways associated with proteins with increased protein expression ratios (PER) in IR⁺ isolates. Isolates 392 and 463 had elevated Mn concentration in their UFs when compared to the founder strain F3



pathways were found for isolates 393 and 463, whereas a number of over-expressed proteins for isolate 393 belonged to pathways not scored for the other 2 isolates. These pathways included arginine and proline metabolism, fatty acid metabolism, geraniol degradation, and gluconeogenesis. In addition, increased ribosome biogenesis was found for isolates 392 and 463, but not 393, which was the isolate with the lowest number of over-expressed proteins.

Discussion

To investigate metabolic routes contributing to the extreme radiation resistance of the halophilic archaeon *H. salinarum*, we selected for super-resistant (IR⁺) isolates by subjecting cultures of *H. salinarum* to successive rounds of high-level IR exposure followed by recovery. Two strains of IR⁺ *H. salinarum* were previously isolated after 4 rounds of high-level IR with a D_{10} of ~12 kGy (DeVeaux et al. 2007). Here we obtained 30 IR⁺ isolates of *H. salinarum* with a D_{10} of ~17 kGy after 6 and 9 rounds of high-level IR exposure; three of these isolates were further characterized using biochemical and proteomic tools.

Role of Mn-antioxidant complexes in enhanced IR resistance

The contribution of non-enzymatic processes in the radiation resistance of bacteria and archaea, and the key role Mn-antioxidant complexes play in scavenging IR-generated ROS have been previously established (Daly et al. 2010; Robinson et al. 2011; Webb and DiRuggiero 2012). Using a similar in vitro assay, we showed that the enzyme-free cell extracts (UFs) of *H. salinarum* IR⁺ isolates protected protein activity from IR to doses significantly higher than with the founder strain. The significant increase in intracellular Mn (between 15 and 30 μ M) of 2 IR⁺ isolates, when compared to the founder, supported the major role for Mn antioxidants in IR resistance in *H. salinarum* and in the enhanced resistance of these strains. Similarly, the addition of 25 μ M Mn to the UF of the hyperthermophilic archaeon, *P. furiosus*, increased enzyme protection by more than 1 kGy, in vitro, and the protection afforded by mannosylglycerate by more than 3 kGy (Webb and DiRuggiero 2012). Daly et al. (2010) also showed that protection of protein activity rose from 10 to 22.5 kGy when 200 μ M of Mn was added to a mixture of phosphate buffer and decapeptides.

Biochemical analysis of the UFs revealed a large increase in free amino acids in isolate 392, mostly the result of glycine accumulation in the cell. Amino acids and small peptides have been shown to have ROS-scavenging capabilities in vitro and in vivo (Wu et al. 2003; Mendis

et al. 2005; Peng et al. 2009; Sheih et al. 2009) and it suggests that, in isolate 392, the combination of high Mn, PO₄, and glycine might be an important component of the enhanced IR resistance of this strain. While isolate 463 also displayed increased intracellular Mn, this was not the case for isolate 393, indicating that other organic metabolites with radioprotective properties might be found in these cells. There are indeed several examples of metabolites with ROS-scavenging properties among the IR-resistant organisms investigated so far, including amino acids, nucleosides and small peptides (Daly et al. 2010; Robinson et al. 2011), trehalose (Billi et al. 2000; Shirkey et al. 2003; Webb and DiRuggiero 2012), dipicolinic acid (Granger et al. 2011), and mycosporin-like amino acids (Yakovleva et al. 2004; Oren and Gunde-Cimerman 2007). However, any biochemical analyses remain challenging in *H. salinarum* because of the extremely high KCl concentration typically found in these cells (DasSarma and Arora 2001).

Proteomic analysis of IR⁺ isolates

We used a proteomic approach to elucidate the metabolic pathways contributing to the IR⁺ phenotype of our *H. salinarum* isolates. In this analysis, we compared the protein abundances of the IR⁺ isolates to those of the *H. salinarum* founder strain (F3) and found a large number of proteins differentially expressed, potentially contributing to the increased IR⁺ tolerance of the isolates. We selected a proteomic approach to circumvent temporal shifts between transcripts and protein abundance levels previously reported for *H. salinarum* in response to IR (Whitehead et al. 2006). Our iTRAQ analysis identified 1,279 proteins, a 48 % coverage of the predicted *H. salinarum* proteome, which fell within the range of previous iTRAQ studies (39–63 %) (Whitehead et al. 2006; Van et al. 2008). The physical characteristics (molecular weight, isoelectric point) and metabolic classification of the proteins we identified were similar to the predicted proteome of *H. salinarum*, indicating little bias in our analysis for most protein functional categories. The exceptions were membrane and transport proteins and this was likely an artifact of the protein extraction method we used. A similar trend was also reported in previous proteomic studies with *H. salinarum* (Van et al. 2008; Goo et al. 2003). Protein expression ratios (PERs) were calculated for each protein to detect differential expression between isolates and the founder strain.

Overall, the IR⁺ isolates had far less protein with decreased PER than increased PER. This was a limitation of the method, as proteins absent, or with expression levels below the detection limit of the method, were not represented in the proteomic dataset. The majority of proteins under-expressed were gas vesicle proteins. Gas vesicles are

protein complexes that accumulate gases through the hydrophobic exclusion of water, providing buoyancy to the cell (Chu et al. 2011). In *H. salinarum*, these proteins are expressed from two gene clusters containing 14 genes (Yao and Facciotti 2011). GvpC is a structural protein, and GvpO is a regulatory transcription protein for one of the gene clusters (Chu et al. 2011). All three isolates had decreased PER for the GvpC and GvpO proteins, indicating a disruption in gas vesicle synthesis, which was confirmed by the observed gas vesicle-deficient phenotype of the IR⁺ isolates. One of the 2 IR⁺ mutant strains previously isolated was also gas vesicle-deficient (DeVeaux et al. 2007). Importantly, we showed that a gas vesicle-deficient mutant for the founder strain was not more radiation-resistant than the wild-type, ruling out a role for gas vesicles in IR resistance.

Effects of Mn accumulation on metabolic pathways

Isolates 392 and 463 accumulated significantly more Mn in their UFs than the founder strain, suggesting that the effect of intracellular Mn on cellular processes and energy metabolism might contribute to the enhanced IR resistance observed in these isolates. While the accumulation of antioxidant Mn-complexes can confer radioprotection to the cell, Mn can also enhance oxidative stress resistance by substituting as a cofactor for iron in certain enzymes susceptible to oxidative attack (Sobota and Imlay 2011). In addition, a number of studies in bacteria reported stimulation of carbon metabolism by elevated intracellular Mn (Horsburgh et al. 2002; Kehres and Maguire 2003; Ogunniyi et al. 2010; Puri et al. 2010), implying that the activation of enzymes involved in energy metabolism we observed in our IR⁺ mutants might be mediated by high-cellular Mn.

Regulation of Mn transport

No Nramp-type Mn transporter has been identified in the genome of *H. salinarum* but deletion of the Mn ABC-transporter genes *zurA*, *zurM*, and *ycdH* did not result in a defective growth phenotype, suggesting an alternative transport system for Mn (Kaur et al. 2006). The ZurA, ZurM, and YcdH proteins were not present in our proteomic dataset but several other transport proteins were over-expressed in 392 and 463 isolates, including a hypothetical K⁺ transporter with a putative cellular function for Mn ion-binding and an ArgK-type transport ATPase involved in the phosphorylation of periplasmic binding proteins of the lysine, arginine, ornithine transport system (Celis 1990). Previous transcriptomic and proteomic studies with *H. salinarum* provided some insights on the regulatory control of Mn homeostasis (Kaur et al. 2006; Bonneau et al. 2007).

The putative Mn-dependent autorepressor SirR, an MntR family regulator, was found to repress the Mn uptake ABC-transport system and a *sirR* deletion resulted in the activation of Mn and phosphate transport genes, poor growth under Mn stress, and the activation of siderophore biosynthesis (Bonneau et al. 2007). In agreement with these findings, we did not find over-expression of the SirR protein in any of the mutant. However, the Mn-induced Fe-deficiency in *H. salinarum* suggests the presence of a still unknown regulator inhibited by high-intracellular Mn (Kaur et al. 2006). Furthermore, recent work with the yeast *S. cerevisiae* presented evidence that intracellular Mn was tightly regulated through nutrient sensing pathways and that it was an integral part of a system level oxidative stress defense in this organism (Reddi and Culotta 2011).

Role of RPA proteins in enhanced resistance to IR

While the current model regarding IR resistance is based on the cell's ability to protect its proteins from IR-induced oxidation (Daly 2012), it is remarkable that two proteins over-expressed in all the IR⁺ isolates were the replication factor A proteins (RPAs) Rfa3 and Rfa8. RPAs, also called single-strand binding proteins, bind to single-stranded DNA (ssDNA) with high affinity and provide protection against nuclease and chemical attacks. RPAs are essential for DNA metabolism, including DNA replication, recombination, and repair in all domains of life (Wold 1997). Two operons, *RpaA1* and *RpaA3* (including *rfa3* and *rfa8*), and a single gene, *rfa1* encode RPA proteins in *H. salinarum* (Webb and DiRuggiero 2013). Using quantitative RT-PCR, we found over-expression of the *rfa3* and *rfa1* genes in a number of *H. salinarum* IR⁺ strains from our collection (DiRuggiero, unpublished). Increased mRNA levels for *rfa3* and *rfa8* were also reported for *H. salinarum* IR⁺ mutants (DeVeaux et al. 2007). In addition, the *Rpa3* operon was induced in response to gamma radiation and UV-C in *H. salinarum* (Baliga et al. 2004; Whitehead et al. 2006) and more recently, two studies reported the hypersensitivity to DNA damaging agents of a *rfa3* homologs (*rpaB*) knock out mutant in *H. volcanii* (Skowrya and MacNeill 2012; Stroud et al. 2012). Constructs over-expressing the *H. volcanii* RpaC protein (Rfa1 homolog) exhibited increased survival to UV-C, MMS, and phleomycin exposure (Skowrya and MacNeill 2012). These studies and our data clearly implicate RPAs in enhanced survival to DNA-damaging treatments.

High doses of IR produce a large number of DNA DSBs, increasing the amount of ssDNA, the substrate for homologous recombination repair (Kish and DiRuggiero 2008; Slade and Radman 2011). In IR⁺ isolates, the high steady-state expression of RPA proteins likely protects ssDNA from degradation, facilitating repair, and ultimately

enhancing cell survival Although it remains to be demonstrated, we propose that increased levels of RPA proteins enhance survival of damaged cells by attending to the increase in ssDNA targets produced by irradiation.

Conclusion

Our biochemical analysis of IR⁺ mutants of *H. salinarum*, evolved over multiple cycles of exposure to high doses of IR, confirmed the key role for Mn antioxidants in the IR resistance of this organism. Analysis of the proteome of *H. salinarum* IR⁺ mutants revealed increased expression for proteins involved in energy metabolism, replenishing the cell with reducing equivalents depleted by the oxidative stress inflicted by IR. Maintenance of redox homeostasis was also activated by the over-expression of coenzyme biosynthesis pathways involved in redox reactions. We conclude here that the increased tolerance to IR observed in the *H. salinarum* mutants is a combination of metabolic regulatory adjustments and the accumulation of Mn-antioxidant complexes.

Acknowledgments This work was supported by the AFOSR (Grant FA95500710158) to J. DiRuggiero. The authors thank Elena Gaidamakova and Vera Matrosova at the Uniformed Services University of the Health Sciences (USUHS) for their technical support using the gamma source at USUHS and M. J. Daly for his support.

References

- Al-Maghrebi M, Fridovich I, Benov L (2002) Manganese supplementation relieves the phenotypic deficits seen in superoxide-dismutase-null *Escherichia coli*. Arch Biochem Biophys 402:104–109
- Archibald FS, Fridovich I (1982) Investigations of the state of the manganese in *Lactobacillus plantarum*. Arch Biochem Biophys 215:589–596
- Baliga NS, Bjork SJ, Bonneau R, Pan M, Iloanusi C, Kottemann MC, Hood L, DiRuggiero J (2004) Systems level insights into the stress response to UV radiation in the halophilic archaeon *Halobacterium* NRC-1. Genome Res 14:1025–1035
- Barnese K, Gralla EB, Cabelli DE, Valentine JS (2008) Manganous phosphate acts as a superoxide dismutase. J Am Chem Soc 130:4604–4606
- Billi D, Friedmann EI, Hofer KG, Grilli Caiola M, Ocampo-Friedmann R (2000) Ionizing-radiation resistance in the desiccation-tolerant cyanobacterium *Chroococcidiopsis*. Appl Environ Microbiol 66:1489–1492
- Bonneau R, Facciotti MT, Reiss DJ, Schmid AK, Pan M, Kaur A, Thorsson V, Shannon P, Johnson MH, Bare JC, Longabaugh W, Vuthoori M, Whitehead K, Madar A, Suzuki L, Mori T, Chang DE, DiRuggiero J, Johnson CH, Hood L, Baliga NS (2007) A predictive model for transcriptional control of physiology in a free living cell. Cell 131:1354–1365
- Celis RT (1990) Mutant of *Escherichia coli* K-12 with defective phosphorylation of two periplasmic transport proteins. J Biol Chem 265:1787–1793
- Chang EC, Kosman DJ (1989) Intracellular Mn(II)-associated superoxide scavenging activity protects Cu, Zn superoxide dismutase-deficient *Saccharomyces cerevisiae* against dioxygen stress. J Biol Chem 264:12172–12178
- Chu LJ, Chen MC, Setter J, Tsai YS, Yang H, Fang X, Ting YS, Shaffer SA, Taylor GK, von Haller PD, Goodlett DR, Ng WV (2011) New structural proteins of *Halobacterium salinarum* gas vesicle revealed by comparative proteomics analysis. J Proteome Res 10:1170
- Confalonieri F, Sommer S (2011) Bacterial and archaeal resistance to ionizing radiation. J Phys Conf Series 261. doi:10.1088/1742-6596/1261/1081/012005
- Daly MJ (2009) A new perspective on radiation resistance based on *Deinococcus radiodurans*. Nat Rev Microbiol 7:237–245
- Daly MJ (2012) Death by protein damage in irradiated cells. DNA Repair 11:12–21
- Daly MJ, Gaidamakova EK, Matrosova VY, Vasilenko A, Zhai M, Leapman RD, Lai B, Ravel B, Li SM, Kemner KM, Fredrickson JK (2007) Protein oxidation implicated as the primary determinant of bacterial radioresistance. PLoS Biol 5:e92
- Daly MJ, Gaidamakova EK, Matrosova VY, Kiang JA, Fukumoto R, Lee D-Y, Wehr NB, Viteri GA, Berlett BS, Levine RL (2010) Small-molecule antioxidant proteome-shields in *Deinococcus radiodurans*. PLoS One 5:e12570
- DasSarma S, Arora P (2001) Halophiles. In: Encyclopedia of life sciences, Nature Publishing Group, pp 1–9
- Davies R, Sinskey AJ (1973) Radiation-resistant mutants of *Salmonella typhimurium* LT2: development and characterization. J Bacteriol 113:133–144
- DeVeaux LC, Iler JA, Smith J, Petrisko J, Wells DP, DasSarma S (2007) Extremely radiation-resistant mutants of a halophilic archaeon with increased single-stranded DNA-binding protein (RPA) gene expression. Radiation Res 168:507–514
- Du J, Gebicki JM (2004) Proteins are major initial cell targets of hydroxyl free radicals. Int J Biochem Cell Biol 36:2334–2343
- Fredrickson JK, Li SM, Gaidamakova EK, Matrosova VY, Zhai M, Sulloway HM, Scholten JC, Brown MG, Balkwill DL, Daly MJ (2008) Protein oxidation: key to bacterial desiccation resistance? ISME J 2:393–403
- Goo YA, Yi EC, Baliga NS, Tao WA, Pan M, Aebersold R, Goodlett DR, Hood L, Ng WV (2003) Proteomic analysis of an extreme halophilic archaeon, *Halobacterium* sp. NRC-1. Mol Cell Proteomics 2(8):506–524
- Granger AC, Gaidamakova EK, Matrosova VY, Daly MJ, Setlow P (2011) Effects of Mn and Fe levels on *Bacillus subtilis* spore resistance and effects of Mn²⁺, other divalent cations, orthophosphate, and dipicolinic acid on protein resistance to ionizing radiation. Appl Environ Microbiol 77:32–40
- Harris DR, Pollock SV, Wood EA, Goiffon RJ, Klingele AJ, Cabot EL, Schackwitz W, Martin J, Eggington J, Durfee TJ, Middle CM, Norton JE, Popelars MC, Li H, Klugman SA, Hamilton LL, Bane LB, Pennacchio LA, Albert TJ, Perna NT, Cox MM, Battista JR (2009) Directed evolution of ionizing radiation resistance in *Escherichia coli*. J Bacteriol 191:5240–5252
- Horsburgh MJ, Wharton SJ, Karavolos M, Foster SJ (2002) Manganese: elemental defence for a life with oxygen. Trends Microbiol 10:496–501
- Imlay JA (2003) Pathways of oxidative damage. Annu Rev Microbiol 57:395–418
- Imlay JA (2006) Iron-sulphur clusters and the problem with oxygen. Mol Microbiol 59:1073–1082
- Imlay JA (2008) Cellular defenses against superoxide and hydrogen peroxide. Annu Rev Biochem 77:755–776
- Kaur A, Pan M, Meislin M, Facciotti MT, El-Gewely R, Baliga NS (2006) A systems view of haloarchaeal strategies to withstand stress from transition metals. Genome Res 16:841–854

- Kaur A, Van PT, Busch CR, Robinson CK, Pan M, Pang WL, Reiss D, DiRuggiero J, Baliga NS (2010) Coordination of frontline defense mechanisms under severe oxidative stress. *Mol Syst Biol* 393: doi:[10.1038/msb.2010.1050](https://doi.org/10.1038/msb.2010.1050)
- Kehres DG, Maguire ME (2003) Emerging themes in manganese transport, biochemistry and pathogenesis in bacteria. *FEMS Microbiol Rev* 27:263–290
- Kennedy SP, Ng WV, Salzberg SL, Hood L, DasSarma S (2001) Understanding the adaptation of *Halobacterium* Species NRC-1 to its extreme environment through computational analysis of its genome sequence. *Genome Res* 11:1641–1650
- Kish A, DiRuggiero J (2008) Rad50 is not essential for the Mre11-dependent repair of DNA double-strand breaks in *Halobacterium* sp. strain NRC-1. *J Bacteriol* 190:5210–5216
- Kish A, Kirkali G, Robinson C, Rosenblatt R, Jaruga P, Dizdaroglu M, DiRuggiero J (2009) Salt shield: intracellular salts provide cellular protection against ionizing radiation in the halophilic archaeon, *Halobacterium salinarum* NRC-1. *Environ Microbiol* 11:1066
- Kish A, Griffin PL, Rogers KL, Fogel ML, Hemley RJ, Steele A (2012) High-pressure tolerance in *Halobacterium salinarum* NRC-1 and other non-piezophilic prokaryotes. *Extremophiles* 16:355–361
- Kottemann M, Kish A, Iloanusi C, Bjork S, DiRuggiero J (2005) Physiological responses of the halophilic archaeon *Halobacterium* sp. strain NRC1 to desiccation and gamma irradiation. *Extremophiles* 9:219–227
- Markillie LM, Varnum SM, Hradecky P, Wong KK (1999) Targeted mutagenesis by duplication insertion in the radioresistant bacterium *Deinococcus radiodurans*: radiation sensitivities of catalase (*katA*) and superoxide dismutase (*sodA*) mutants. *J Bacteriol* 181:666–669
- McNaughton RL, Reddi AR, Clement MH, Sharma A, Barnese K, Rosenfeld L, Gralla EB, Valentine JS, Culotta VC, Hoffman BM (2010) Probing in vivo Mn²⁺ speciation and oxidative stress resistance in yeast cells with electron-nuclear double resonance spectroscopy. *Proc Natl Acad Sci USA* 107:15335–15339
- Mendis E, Rajapakse N, Kim SK (2005) Antioxidant properties of a radical-scavenging peptide purified from enzymatically prepared fish skin gelatin hydrolysate. *J Agric Food Chem* 53:581–587
- Nauser T, Koppenol WH, Gebicki JM (2005) The kinetics of oxidation of GSH by protein radicals. *Biochem J* 392:693–701
- Ogunniyi AD, Mahdi LK, Jennings MP, McEwan AG, McDevitt CA, Van der Hoek MB, Bagley CJ, Hoffmann P, Gould KA, Paton JC (2010) Central role of manganese in regulation of stress responses, physiology, and metabolism in *Streptococcus pneumoniae*. *J Bacteriol* 192:4489–4497
- Oren A, Gunde-Cimerman N (2007) Mycosporines and mycosporine-like amino acids: UV protectants or multipurpose secondary metabolites? *FEMS Microbiol Lett* 269:1–10
- Peng X, Xiong YL, Kong B (2009) Antioxidant activity of peptide fractions from whey protein hydrolysates as measured by electron spin resonance. *Food Chem* 113:196–201
- Puri S, Hohle TH, O'Brian MR (2010) Control of bacterial iron homeostasis by manganese. *Proc Natl Acad Sci USA* 107:10691
- Reddi AR, Culotta VC (2011) Regulation of manganese antioxidants by nutrient sensing pathways in *Saccharomyces cerevisiae*. *Genetics* 189:1261–1270
- Riley PA (1994) Free radicals in biology: oxidative stress and the effects of ionizing radiation. *Int J Radiat Biol* 65:27–33
- Robinson CK, Webb K, Kaur A, Jaruga P, Dizdaroglu M, Baliga NS, Place A, DiRuggiero J (2011) A major role for nonenzymatic antioxidant processes in the radioresistance of *Halobacterium salinarum*. *J Bacteriol* 193:1653–1662
- Scott MD, Meshnick SR, Eaton JW (1989) Superoxide dismutase amplifies organismal sensitivity to ionizing radiation. *J Biol Chem* 264:2498–2501
- Sheih IC, Wu TK, Fang TJ (2009) Antioxidant properties of a new antioxidative peptide from algae protein waste hydrolysate in different oxidation systems. *Bioresour Technol* 100:3419–3425
- Shirkey B, McMaster NJ, Smith SC, Wright DJ, Rodriguez H, Jaruga P, Birincioglu M, Helm RF, Potts M (2003) Genomic DNA of *Nostoc commune* (Cyanobacteria) becomes covalently modified during long-term (decades) desiccation but is protected from oxidative damage and degradation. *Nucleic Acids Res* 31:2995–3005
- Skowrya A, MacNeill SA (2012) Identification of essential and non-essential single-stranded DNA-binding proteins in a model archaeal organism. *Nucleic Acids Res* 40:1077–1090
- Slade D, Radman M (2011) Oxidative stress resistance in *Deinococcus radiodurans*. *Microbiol Mol Biol Rev* 75:133
- Slade D, Lindner AB, Paul G, Radman M (2009) Recombination and replication in DNA repair of heavily irradiated *Deinococcus radiodurans*. *Cell* 136:1044–1055
- Sobota JM, Imlay JA (2011) Iron enzyme ribulose-5-phosphate-3-epimerase in *Escherichia coli* is rapidly damaged by hydrogen peroxide but can be protected by manganese. *Proc Natl Acad Sci USA* 108:5402–5407
- Stroud A, Liddell S, Allers T (2012) Genetic and biochemical identification of a novel single-stranded DNA-binding complex in *Haloflex volcanii*. *Frontiers Microbiol* 3:224
- Van PT, Schmid AK, King NL, Kaur A, Pan M, Whitehead K, Koide T, Facciotti MT, Goo YA, Deutsch EW, Reiss DJ, Mallick P, Baliga NS (2008) *Halobacterium salinarum* NRC-1 PeptideAtlas: toward strategies for targeted proteomics and improved proteome coverage. *J Proteome Res* 7:3755–3764
- Webb KM, DiRuggiero J (2012) Role of Mn²⁺ and compatible solutes in the radiation resistance of thermophilic bacteria and archaea. *Archaea*. Article ID 845756. doi:[10.1155/2012/845756](https://doi.org/10.1155/2012/845756)
- Webb KM, DiRuggiero J (2013) Radiation resistance in extremophiles: fending off multiple attacks. In: Seckbach J, Oren A, Stan-Lotter H (eds) *Polyextremophiles: life under multiple forms of stress*. Series: cellular origin, life in extreme habitats and astrobiology, vol 27. Springer, Dordrecht. doi:[10.1007/978-94-007-6488-0_10](https://doi.org/10.1007/978-94-007-6488-0_10)
- Whitehead K, Kish A, Pan M, Kaur A, Reiss DJ, King N, Hohmann L, DiRuggiero J, Baliga NS (2006) An integrated systems approach for understanding cellular responses to gamma radiation. *Mol Syst Biol* 47. doi:[10.1038/msb4100091](https://doi.org/10.1038/msb4100091)
- Wold MS (1997) Replication protein A: a heterotrimeric, single-stranded DNA-binding protein required for eukaryotic DNA metabolism. *Annu Rev Biochem* 66:61–92
- Wu HC, Chen HM, Shiau CY (2003) Free amino acids and peptides as related to antioxidant properties in protein hydrolysates of mackerel (*Scomber austriasicus*). *Food Res Intern* 36:949–957
- Yakovleva I, Bhagooli R, Takemura A, Hidaka M (2004) Differential susceptibility to oxidative stress of two scleractinian corals: antioxidant functioning of mycosporine-glycine. *Comp Biochem Physiol B Biochem Mol Biol* 139:721–730
- Yao AI, Facciotti MT (2011) Regulatory multidimensionality of gas vesicle biogenesis in *Halobacterium salinarum* NRC-1. *Archaea*. Article ID 716456